Photon-Mediated Localization in Two-Level Qubit Arrays

Janet Zhong,[1] Nikita A. Olekhno,[2] Yongguan Ke,[1,3] Alexander V. Poshakinskiy,[4] Chaohong Lee,[3,5] Yuri S. Kivshar,[1,2] and Alexander N. Poddubny[1,2,4,*]

[1]*Nonlinear Physics Centre, Research School of Physics, Australian National University, Canberra ACT 2601, Australia*
[2]*ITMO University, St. Petersburg 197101, Russia*
[3]*Guangdong Provincial Key Laboratory of Quantum Metrology and Sensing & School of Physics and Astronomy, Sun Yat-Sen University (Zhuhai Campus), Zhuhai 519082, China*
[4]*Ioffe Institute, St. Petersburg 194021, Russia*
[5]*State Key Laboratory of Optoelectronic Materials and Technologies, Sun Yat-Sen University (Guangzhou Campus), Guangzhou 510275, China*

(Received 22 November 2019; accepted 10 February 2020; published 5 March 2020)

We predict the existence of a novel interaction-induced spatial localization in a periodic array of qubits coupled to a waveguide. This localization can be described as a quantum analogue of a self-induced optical lattice between two indistinguishable photons, where one photon creates a standing wave that traps the other photon. The localization is caused by the interplay between on-site repulsion due to the photon blockade and the waveguide-mediated long-range coupling between the qubits.

DOI: 10.1103/PhysRevLett.124.093604

Introduction.—Many-body quantum optical systems have received intense interest in recent years due to ground-breaking experiments with superconducting qubits [1–3] and cold atoms coupled to waveguides [4]. A paradigmatic system in quantum optics is an array of atoms coupled to freely propagating photons [5–7]. Waveguide quantum electrodynamics, where photons propagate in one dimension, is promising for quantum networks [8] and quantum computation [9]. When atoms are located at the same point, the full quantum problem can be solved exactly [10] because light interacts only with the symmetric superradiant excitation of the array. When atoms are arranged in a lattice where the spacing is smaller than the wavelength of incident light, collective subradiant excitations begin to play an important role [11–15].

The physics of such systems becomes especially rich in the multiexcitation regime due to photon blockade. Since a single qubit cannot be excited twice, the interaction between excitations becomes a decisive factor that strongly affects both the lifetime and spatial distribution of the collective many-body states. For arrays of two-level atoms, subradiant two-excitation states are fermionized due to interactions [16] and two-particle excitations which are products of dark and bright single-excitation states can appear [17]. Spatially bound subradiant dimers have also been predicted [18] and a transition from few-body quantum to nonlinear classical regimes has recently been theorized [19].

In this Letter, we uncover and study a new class of two-particle hybrid excitations in arrays of subwavelength-spaced two-level qubits coupled to a waveguide. We reveal that when one of two indistinguishable photons forms a standing wave, the second photon can be localized in the nodes of this wave, as shown in Fig. 1(a). This effect can be viewed as a self-induced quantum optical lattice. This state is represented as a special type of photon-mediated cross-shaped states with strong spatial localization in the quasi-2D probability distribution, as in Figs. 1(b) and 1(c). In the quasi-2D color map Fig. 1(b) the x and y coordinates correspond to the positions of the first and second excitations, and the color represents the probability of a pair to occupy that site. The "cross shape" means that the motion is highly constrained for the first excitation and free to propagate in space for the second excitation, or vice versa. We demonstrate that such cross-shaped states arise naturally for subwavelength arrays in a broad range of

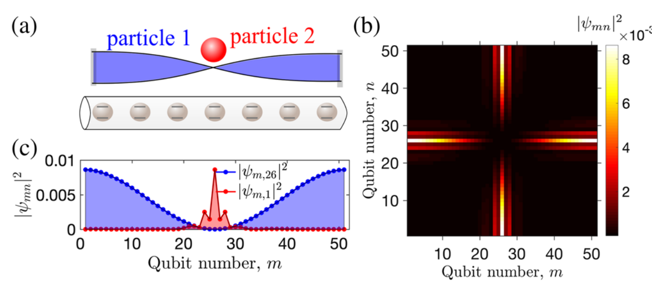

FIG. 1. (a) Schematic illustration of a two-particle state in an array of qubits in a waveguide, where one photon behaves as a standing wave and traps another one in the antinode of that wave. (b) Spatial map of the corresponding two-excitation wave function $|\psi_{mn}|^2$ with $\varepsilon/\Gamma_0 = -2.57 - 0.54i$ depending on the coordinates of the first and second qubits. (c) Cross sections of the map for $n = 1$ and 26. The calculation parameters are $\varphi = 0.01$, $N = 51$, $\chi = 0.5 \times 10^3 \Gamma_0$.

parameters which should be experimentally observable in systems where the qubits are probed individually [3].

In the single-excitation regime for the same system, all single-particle states are ordinary delocalized standing waves. Thus, the presence of strong localization on just a few lattice sites in the two-excitation regime, as observed in Fig. 1(b), is solely a result of the interaction due to photon blockade. While the most subradiant excitations in the considered system behave as hard-core bosons [16], the ansatz of Ref. [16] involves only single-particle states that are delocalized and do not describe our cross-shaped states. Since the localization involves two indistinguishable entangled particles, it is also qualitatively different from the physics of self-localized polarons which originates from electron-phonon interaction in solids.

The spatially localized structure studied in this Letter bears some resemblance to the profiles of intrinsic localized modes known to occur in discrete systems [20], self-trapped localized solitons studied in nonlinear discrete systems [21], compact localized states in tight-binding models with flat bands [22], as well as localized excitations found in generalized Bose-Hubbard models [23,24]. However, in our system both long-range coupling and photon blockade are crucial for localization which distinguishes it from these studies. The range of interaction can be tuned in practice by varying the relative strength of the near-field dipole-dipole coupling and the long-distance radiative coupling via the waveguide mode [4,15].

Model and numerical results.—We consider N periodically spaced qubits in a one-dimensional waveguide. In the Markovian approximation, this system is characterized by the Hamiltonian [14,17] (see also Supplemental Material [25] for details)

$$\mathcal{H}=\sum_{m,n}H_{m,n}b_m^\dagger b_n+\frac{\chi}{2}\sum_n b_n^\dagger b_n^\dagger b_n b_n, \qquad (1)$$

where $H_{mn}\equiv -\mathrm{i}\Gamma_0 e^{i\varphi|m-n|}$, $m,n=1\ldots N$. Here, b_m are the annihilation operators for the bosonic excitations of the qubits and the parameter χ describes the interaction. The results for two-level qubits can be obtained in the limit of $\chi/\Gamma_0\to\infty$. The phase $\varphi=q_0 d$ is given by the product of the distance between the qubits d and the light wave vector q_0 at the qubit frequency. The parameter Γ_0 is the radiative decay rate of an individual qubit. We analyze the spatial distribution of the two-excitation states $\sum\psi_{mn}b_n^\dagger b_m^\dagger|0\rangle$ in the strongly subwavelength regime with $0<\varphi\ll 1$ by means of full diagonalization. In the limit of $\chi\to\infty$, when $\psi_{nn}\equiv 0$, the Schrödinger equation can be presented in the following matrix form [25]:

$$H\psi+\psi H-2\mathrm{diag}[\mathrm{diag}(H\psi)]=2\varepsilon\psi, \qquad (2)$$

with $\psi_{nm}=\psi_{mn}$. Here, the first two terms in the left-hand side describe the propagation of the first and second particle, respectively, and the third term accounts for the interaction.

Our numerical calculation demonstrates that a large number of two-excitation states of the system Eq. (2) have the following structure:

$$\psi_{nm}\approx u_n^{(\mathrm{loc})}u_m^{(\mathrm{free})}+u_m^{(\mathrm{loc})}u_n^{(\mathrm{free})}. \qquad (3)$$

Here, the N-vector $u_m^{(\mathrm{free})}$ is essentially a standing wave with the wave vector on the order of π/N, slightly modified by the interaction. The vector $u_n^{(\mathrm{loc})}$ has a very different shape and consists of peaks localized at just several sites which are pinned to the antinodes of the standing wave $u_m^{(\mathrm{free})}$. Examples of several such states are presented in Figs. 2(a)–2(c). Figure 2(d) shows how the number of cross-shaped states of the type of Eq. (3) depends on the distance between the qubits and the interaction strength. The states were singled out by requiring the inverse participation ratios (IPRs) $\sum|u|^4/(\sum|u|^2)^2$ for $u^{(\mathrm{loc})}$ to be larger than 0.12 and the remaining singular values in the Schmidt decomposition to be smaller than 0.25. Physically, large IPR $\lesssim 1$ for $u^{(\mathrm{loc})}$ corresponds to a highly localized state, while delocalized states are characterized by a small IPR $\sim 1/N$. We have also required the IPR of the Fourier transform $\sum_{n=1}^N e^{ikn}u_n^{(\mathrm{free})}$, evaluated for k changing from 0 to π with the step 0.1 to be larger than 0.12 to select free-space solutions. The crosslike states occupy up to 25% of the two-excitation spectrum when the phase is close to an

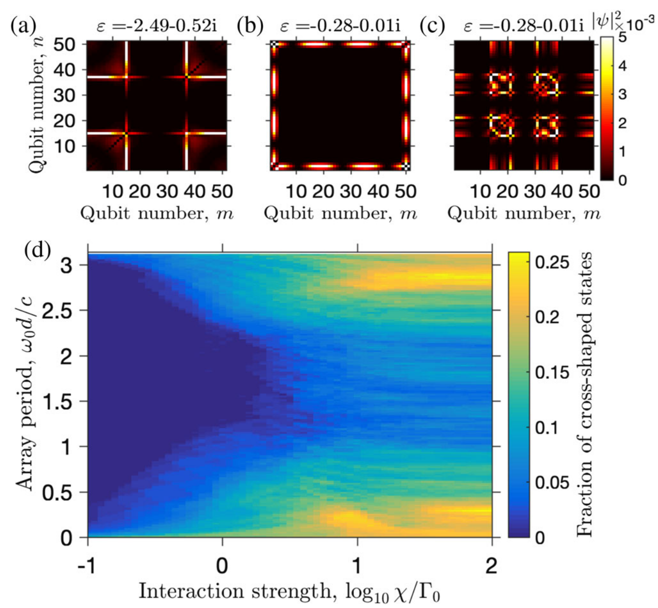

FIG. 2. (a)–(c) Examples of spatial distributions for different two-excitation states calculated for $N=51$ and $\varphi=0.01$. Complex eigenenergy is shown for each panel. (d) Phase diagram showing the relative number of cross-shaped states Eq. (3) depending on the interqubit phase $\varphi=\omega_0 d/c$ and the interaction strength χ. Calculated for $N=25$.

integer multiple of π and when the photon-photon interaction is strong such that $\chi \gg \Gamma_0$.

Quasiflat polaritonic dispersion.—We focus on the crosslike state shown in Fig. 1. It is instructive to first review the results for single-particle states in an infinite periodic array $\sum_n e^{ikn}\sigma_n^\dagger|0\rangle$, where k is the Bloch wave vector. These states are coupled light-matter excitations (polaritons) and their energy dispersion is given by $\varepsilon(k) = \Gamma_0 \sin\varphi/(\cos k - \cos\varphi)$ [26]. The dispersion consists of upper and lower polariton branches separated by the gap around the qubit resonant frequency. We are interested only in the states of the lower polaritonic branch in the regime where $\varphi \ll k \ll 1$. In this case, the lower polaritonic branch can be well approximated by $\varepsilon(k) \approx -2\varphi\Gamma_0/k^2$ for $k \ll 1$, as demonstrated by the calculation in Fig. 3(a). The important feature of this dispersion law, which is central for our study is that there is a huge density of states for ε just below zero when the group velocity is small and $dk/d\varepsilon \gg 1$. In other words, the polaritons are heavy and slow, which strongly facilitates their trapping. This single-particle dispersion leads to quite interesting isoenergy contours for a pair of noninteracting polaritons with the given total energy 2ε and the wave vectors k_x, k_y. The isoenergy contour is given by

$$\varepsilon(k_x, k_y) \approx -\varphi\Gamma_0\left(\frac{1}{k_x^2} + \frac{1}{k_y^2}\right), \tag{4}$$

and is plotted in Fig. 3(b) for the average pair energy $\varepsilon = -2.57\Gamma_0$ corresponding to the real part of the complex energy of the state in Fig. 1(b). Crucially, for most points of the isofrequency contour, the group velocity $d\varepsilon/d\mathbf{k}$ is parallel to either the x or y axis. This means that only one of the two photons can propagate in space at the same time, in full agreement with the real space maps of the eigenstates shown in Figs. 1 and 2.

It is instructive to study the wave function shown in Fig. 1 in the reciprocal space. The results are presented in Figs. 3(c) and 3(d). We start by calculating the Fourier transform along only one particle coordinate, $|\sum_n e^{-ikn}\psi_{mn}|^2$ when the second particle position m is either at the center ($m = 26$) or at the edge ($m = 1$). Indeed, the Fourier transform along the center reveals a sharp peak that corresponds to a standing wave with a well-defined wave vector [blue curve in Fig. 3(c)]. The Fourier transform at the edge results in a broad distribution of large wave vectors characteristic for a localized state [red curve in Fig. 3(c)]. The same results can be deduced from the two-dimensional Fourier transform $|\sum_{nm} e^{-ik_x m - ik_y n}\psi_{mn}|^2$ plotted in Fig. 3(d): one of the two polaritons has large wave vector when the other one has a small one, or vice versa.

Interestingly, the numerically obtained properties of the crosslike states seem to be in general agreement with the features of our study of metastable twilight states reported in Ref. [17]. In this Letter, the twilight state is defined as a metastable product of dark and bright states. Here, the crosslike states result from the products of less subradiant states (standing wave) with strongly subradiant states (localized distribution). In this Letter, we focus on the spatial distribution of the two-photon states, rather than their lifetimes, but more details are given in the Supplemental Material [25].

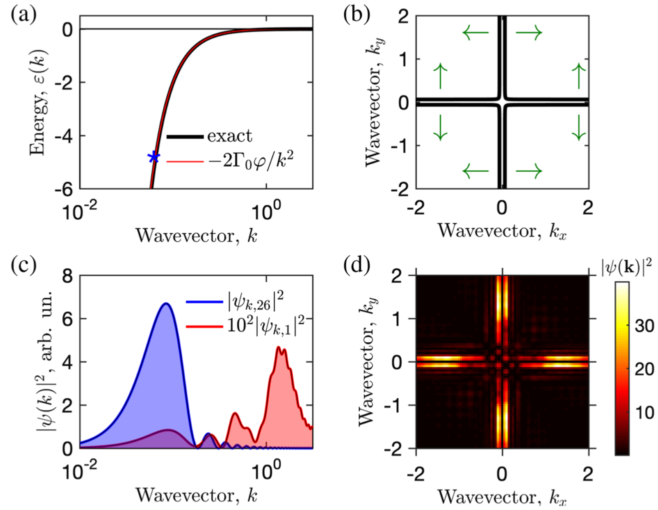

FIG. 3. (a) Lower polariton branch of the single-particle dispersion. Star indicates the energy $\varepsilon = -2 \times 2.57\Gamma_0$ and the wave vector corresponding to the cross-shaped state in Fig. 1. (b) Two-excitation dispersion Eq. (4) for $\varepsilon = -2.57\Gamma_0$. Green arrows indicate the directions of group velocity in the corresponding regions. (c),(d) One- and two-dimensional Fourier transforms of the state ψ_{mn} in Fig. 1. Blue and red curves in (c) are calculated for the m index being at the center or at the edge, respectively. Calculation parameters are the same as in Fig. 1.

Interaction-induced localization.—The flat dispersion is an essential ingredient for the trapping of polaritons. The second necessary ingredient is their interaction. In order to explain the interaction effects analytically we have to overcome the technical difficulty of the original Schrödinger equation, Eq. (2), which has a very dense Hamiltonian for $\varphi \ll 1$, $H_{nm} \approx -i\Gamma_0$ due to the long-range coupling between the qubits. It is useful to write a two-particle equation for the matrix $\mathcal{E} = H\psi H$ rather than the two-photon wave function ψ directly. By rewriting the Schrödinger equation under this transformation (see Ref. [25] for details), we can derive an equation of the form

$$(\partial_x^2 + \partial_y^2)\mathcal{E} - \delta_{x,y}(\partial_x^2 + \partial_y^2)\mathcal{E} = \frac{\varepsilon}{\varphi\Gamma_0}\partial_x^2\partial_y^2\mathcal{E}, \tag{5}$$

where $x, y = 1, N$, and $\partial_{x,y}^2$ are just the operators of discrete second-order derivatives, $\partial_x^2 = \partial^2 \otimes 1_{N\times N}$, $\partial_y^2 = 1_{N\times N} \otimes \partial^2$. The $N \times N$ matrix ∂^2 is defined as

$$\partial^2 \equiv \begin{pmatrix} -1 & 1 & 0 & \dots \\ 1 & -2 & 1 & \dots \\ & & \ddots & \\ \dots & 1 & -2 & 1 \\ \dots & 0 & 1 & -1 \end{pmatrix}. \qquad (6)$$

Importantly, in Eq. (5) we have neglected the radiative decay of the eigenstates, $\mathrm{Im}\varepsilon \equiv 0$, which is a reasonable approximation in the considered strongly subwavelength regime with $\varphi \ll 1$. If the interaction term $\propto \delta_{x,y}$ is omitted, the eigenstates of Eq. (5) are just standing waves with the dispersion law Eq. (4). We have verified numerically that when the interaction term is kept, Eq. (5) features the same kind of cross-shaped eigenstates as our original Schrödinger equation Eq. (2). Hence, while Eq. (5) looks quite simple, it still captures the physics of the interaction-induced localization. Importantly, since the matrices $\partial^2_{x,y}$ are tri-diagonal, Eq. (5) is local in both the first and second photon coordinates x and y. The physical reason why Eq. (5) is local is that the matrix $\mathcal{E}$ describes a two-photon amplitude of the electric field in contrast with the matrix of two-qubit excitations ψ_{mn}. The considered array of qubits is subwavelength and can be viewed as a quantum nonlinear metamaterial [27]. As such, it is natural to expect a local two-photon wave equation in the effective-medium approximation.

In order to explain the localization it remains only to understand why the diagonal cross section of the two-photon distribution $\mathcal{E}(x,x)$ is localized at $x \approx N/2$. To this end, we introduce the Green's function $G(x,y;x',y';\varepsilon)$ of Eq. (5) without the interaction term, satisfying

$$(\partial_x^2 + \partial_y^2)G = \frac{\varepsilon}{\varphi\Gamma_0}\partial_x^2\partial_y^2 G + \delta_{x,x'}\delta_{y,y'}. \qquad (7)$$

The solution of Eq. (7) can be expanded over the single-particle eigensolutions which are just standing waves. We are now interested in the case when the photon pair energy 2ε is close to the resonance of the given standing wave u_0 with the wave vector k_0 and the energy $\varepsilon_0 \approx 2\varepsilon$. The Green's function can then be approximated by the following general expression

$$G(x,y;x',y';\varepsilon) \approx \frac{a}{\delta\varepsilon}[u_0(x)u_0(x')g(y,y') + u_0(y)u_0(y')g(x,x')], \qquad (8)$$

where $\delta\varepsilon = \varepsilon - \varepsilon_0/2$ and $a = \Gamma_0/k_0^2$. Here, the matrix $g(y,y')$ describes the short-range components of the Green's function. By construction, the distribution G as a function of x, y for given x', y' has a crosslike shape which is characteristic of the isoenergy contours discussed in Fig. 3. More detailed derivation and analysis of Eq. (8) is presented in Sec. S3 of the Supplemental Material [25], where we demonstrate that the short-range component can be qualitatively approximated by $g(y,y') \approx [\partial^2 - \kappa^2]^{-1}_{y,y'}$, where $\kappa \sim k_0 \ll 1$ is a cutoff parameter. Physically, the function $g(y,y')$ takes into account the net contribution to the Green's function from all standing waves with the wave vectors larger than k_0.

Substituting Eq. (8) into Eq. (5) we obtain the following equation for the diagonal components of the matrix $\mathcal{E}$:

$$\delta\varepsilon\mathcal{E}(x,x) = \mathcal{L}_{x,x'}\mathcal{E}(x',x'), \qquad (9)$$

where

$$\mathcal{L} = 2a\,\mathrm{diag}[u_0(x)][\partial_x^2 - \kappa^2]^{-1}\mathrm{diag}[u_0(x)]\partial_x^2. \qquad (10)$$

It can be easily checked numerically that for $\kappa \ll 1$ the operator $\mathcal{L}$ has spatially localized eigenstates, see Fig. 4(a). Specifically, the third eigenstate, shown in Fig. 4(b), describes the diagonal cross section of the considered crosslike distribution. Figure 4(c) shows the inverse participation ratio $\sum_x |\psi_x|^4$ for the third eigenstate as a function of the cutoff parameter κ. The high value of IPR ≈ 0.5 for $\kappa \lesssim 0.1$ is a fingerprint of localization. Indeed, for $\kappa \ll 1$ the eigenstate is practically independent of the cutoff parameter and looks like a derivative of a discrete δ function. One can then interpret Eq. (9) as describing a motion of a particle with large mass in the potential determined by $u_0(x)^2 \propto \cos^2(k_0 x)$. Clearly, in such a case the localization takes place in the node of the standing wave $u_0(x)$, in agreement with the results in Fig. 4. More detailed analysis is given in Sec. S4 of Ref. [25]. Just as in the conventional Bose-Hubbard model [28], our results are valid both for strong repulsion and strong attraction between the photons.

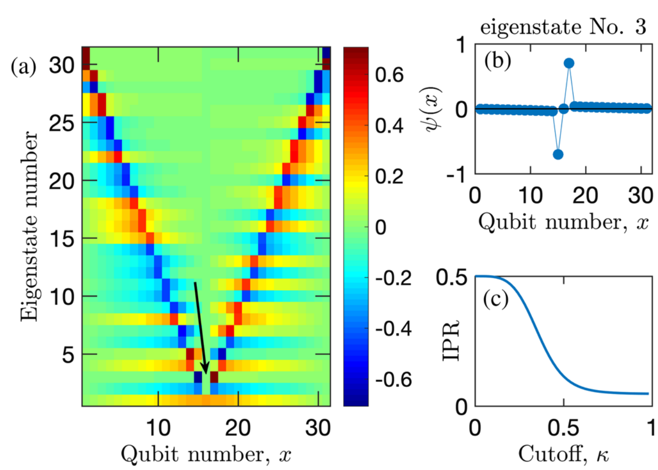

FIG. 4. (a) Eigenstates of the operator (10) for $\kappa = 0.1$, $N = 31$. (b) Spatial profile of the third eigenstate, indicated in (a) by an arrow. Inverse participation ratio of the third eigenstate depending on the cutoff parameter κ.

In summary, we have revealed that the presence of a polariton quantized as standing wave in a finite qubit array creates an effective potential to trap the second polariton. This second polariton is pushed by the repulsive interaction to become localized in the antinodes of the standing wave, and stays trapped there due to its large effective mass. Our finding demonstrates that the interaction yields surprising results in the strongly quantum regime when only several particles are present in the system. We believe that the potential of waveguide quantum electrodynamical platforms for analog quantum simulations of many-body effects is still largely unexplored. For instance, it is not clear whether the considered states can be generalized to the many-body case, such as whether two photons can form an effective two-dimensional optical lattice that can trap the third photon in its nodes. Another open but very interesting question is the role of interactions in topologically nontrivial qubit arrays [29,30].

We acknowledge useful discussions with J. Brehm, M. M. Glazov, L. E. Golub, I. V. Iorsh, E. L. Ivchenko, A. A. Sukhorukov, and A. V. Ustinov. This work was supported by the Australian Research Council. C. L. was supported by the National Natural Science Foundation of China (NNSFC) (Grants No. 11874434 and No. 11574405). Y. K. was partially supported by the Office of China Postdoctoral Council under Grant No. 20180052 and the National Natural Science Foundation of China (NNSFC) under Grant No. 11904419. A. V. P. also acknowledges a partial support from the Russian President Grant No. MK-599.2019.2. A. V. P., A. N. P., and N. A. O. have been partially supported by the Foundation for the Advancement of Theoretical Physics and Mathematics “BASIS.” N. A. O. was supported by the Russian Foundation for Basic Research (Grants No. 18-29-20037 and No. 18-32-01052).

*poddubny@coherent.ioffe.ru

[1] A. F. van Loo, A. Fedorov, K. Lalumiere, B. C. Sanders, A. Blais, and A. Wallraff, Photon-mediated interactions between distant artificial atoms, Science **342**, 1494 (2013).

[2] M. Mirhosseini, E. Kim, X. Zhang, A. Sipahigil, P. B. Dieterle, A. J. Keller, A. Asenjo-Garcia, D. E. Chang, and O. Painter, Cavity quantum electrodynamics with atom-like mirrors, Nature (London) **569**, 692 (2019).

[3] Z. Wang, H. Li, W. Feng, X. Song, C. Song, W. Liu, Q. Guo, X. Zhang, H. Dong, D. Zheng, H. Wang, and D.-W. Wang, Generation and Controllable Switching of Superradiant and Subradiant States in a 10-Qubit Superconducting Circuit, Phys. Rev. Lett. **124**, 013601 (2020).

[4] N. V. Corzo, J. Raskop, A. Chandra, A. S. Sheremet, B. Gouraud, and J. Laurat, Waveguide-coupled single collective excitation of atomic arrays, Nature (London) **566**, 359 (2019).

[5] R. H. Dicke, Coherence in spontaneous radiation processes, Phys. Rev. **93**, 99 (1954).

[6] D. Roy, C. M. Wilson, and O. Firstenberg, Colloquium: Strongly interacting photons in one-dimensional continuum, Rev. Mod. Phys. **89**, 021001 (2017).

[7] D. E. Chang, J. S. Douglas, A. González-Tudela, C.-L. Hung, and H. J. Kimble, Colloquium: Quantum matter built from nanoscopic lattices of atoms and photons, Rev. Mod. Phys. **90**, 031002 (2018).

[8] H. J. Kimble, The quantum internet, Nature (London) **453**, 1023 (2008).

[9] H. Zheng, D. J. Gauthier, and H. U. Baranger, Waveguide-QED-Based Photonic Quantum Computation, Phys. Rev. Lett. **111**, 090502 (2013).

[10] V. Yudson and V. Rupasov, Exact Dicke superradiance theory: Bethe wavefunctions in the discrete atom model, Sov. Phys. JETP **59**, 478 (1984), http://www.jetp.ac.ru/cgi-bin/e/index/e/59/3/p478?a=list.

[11] M. R. Vladimirova, E. L. Ivchenko, and A. V. Kavokin, Exciton polaritons in long-period quantum-well structures, Fiz. Tekh. Poluprovodn. **32**, 90 (1998).

[12] A. N. Poddubny, L. Pilozzi, M. M. Voronov, and E. L. Ivchenko, Resonant Fibonacci quantum well structures in one dimension, Phys. Rev. B **77**, 113306 (2008).

[13] A. N. Poddubny, L. Pilozzi, M. M. Voronov, and E. L. Ivchenko, Exciton-polaritonic quasicrystalline and aperiodic structures, Phys. Rev. B **80**, 115314 (2009).

[14] A. Albrecht, L. Henriet, A. Asenjo-Garcia, P. B. Dieterle, O. Painter, and D. E. Chang, Subradiant states of quantum bits coupled to a one-dimensional waveguide, New J. Phys. **21**, 025003 (2019).

[15] D. F. Kornovan, N. V. Corzo, J. Laurat, and A. S. Sheremet, Extremely subradiant states in a periodic one-dimensional atomic array, Phys. Rev. A **100**, 063832 (2019).

[16] Y.-X. Zhang and K. Mølmer, Theory of Subradiant States of a One-Dimensional Two-Level Atom Chain, Phys. Rev. Lett. **122**, 203605 (2019).

[17] Y. Ke, A. V. Poshakinskiy, C. Lee, Y. S. Kivshar, and A. N. Poddubny, Inelastic Scattering of Photon Pairs in Qubit Arrays with Subradiant States, Phys. Rev. Lett. **123**, 253601 (2019).

[18] Y.-X. Zhang, C. Yu, and K. Mølmer, Subradiant dimer excited states of atom chains coupled to a 1D waveguide, arXiv:1908.01818 [Phys. Rev. Lett. (to be published)].

[19] S. Mahmoodian, G. Calajó, D. E. Chang, K. Hammerer, and A. S. Sørensen, Dynamics of many-body photon bound states in chiral waveguide QED, arXiv:1910.05828.

[20] D. K. Campbell, S. Flach, and Y. S. Kivshar, Localizing energy through nonlinearity and discreteness, Phys. Today **57**, No. 1, 43 (2004).

[21] Y. S. Kivshar, Self-Induced Gap Solitons, Phys. Rev. Lett. **70**, 3055 (1993).

[22] D. Leykam, A. Andreanov, and S. Flach, Artificial flat band systems: From lattice models to experiments, Adv. Phys. X **3**, 1473052 (2018).

[23] S. Longhi and G. Della Valle, Tamm–Hubbard surface states in the continuum, J. Phys. Condens. Matter **25**, 235601 (2013).

[24] M. A. Gorlach and A. N. Poddubny, Topological edge states of bound photon pairs, Phys. Rev. A **95**, 053866 (2017).

[25] See Supplemental Material at http://link.aps.org/supplemental/10.1103/PhysRevLett.124.093604 for details of the two-particle Schrödinger equation (S1), (S2) complex

energy spectrum, (S3) Green's function, (S4) interaction-induced localization, (S5) and time dynamics, which includes a video showing the time dynamics of the two-photon wave function.

[26] E. L. Ivchenko, Excitonic polaritons in periodic quantum-well structures, Sov. Phys. Solid State **33**, 1344 (1991).

[27] P. Macha, G. Oelsner, J.-M. Reiner, M. Marthaler, S. André, G. Schön, U. Hübner, H.-G. Meyer, E. Il'ichev, and A. V. Ustinov, Implementation of a quantum metamaterial using superconducting qubits, Nat. Commun. **5**, 5146 (2014).

[28] K. Winkler, G. Thalhammer, F. Lang, R. Grimm, J. Hecker Denschlag, A. J. Daley, A. Kantian, H. P. Büchler, and P. Zoller, Repulsively bound atom pairs in an optical lattice, Nature (London) **441**, 853 (2006).

[29] A. V. Poshakinskiy, A. N. Poddubny, L. Pilozzi, and E. L. Ivchenko, Radiative Topological States in Resonant Photonic Crystals, Phys. Rev. Lett. **112**, 107403 (2014).

[30] T. Ozawa, H. M. Price, A. Amo, N. Goldman, M. Hafezi, L. Lu, M. C. Rechtsman, D. Schuster, J. Simon, O. Zilberberg, and I. Carusotto, Topological photonics, Rev. Mod. Phys. **91**, 015006 (2019).